

Method to Identify and Visualize Barriers in a Low-Stress Bike Network

Theja Putta¹ and Peter G. Furth¹

Transportation Research Record

1–9

© National Academy of Sciences:

Transportation Research Board 2019

Article reuse guidelines:

sagepub.com/journals-permissions

DOI: 10.1177/0361198119847617

journals.sagepub.com/home/trr



Abstract

Low-stress bike networks are often disconnected, with gaps or barriers that make travel between two points impossible without riding on high-stress roads. Barriers can also force long detours that people are not willing to make. Although existing methods of low-stress bike network analysis have been used to point out some barriers, a method was needed to systematically identify and draw barriers to assist in network planning. Such a method was developed, taking only the low-stress network as an input, and yielding a set of polylines that indicated barriers to bicycling. Applications in Arlington, Virginia and Boston, Massachusetts showed how it detected what might otherwise have been hidden barriers. The method also successfully highlighted critical low-stress links that breached what would otherwise have been a far longer barrier.

Most urban street networks are dense and offer motor vehicle users redundancy in connecting origins to destinations. The same cannot be said for bicycle networks, if the bicycling network is limited to segments with low traffic stress. In many cities, the low-stress bicycling network is disconnected, with gaps that may completely cut off an origin from many destinations, or require a circuitous path. When a gap extends wider than a level of detour most cyclists will accept, it becomes a barrier to the connectivity of the bike network. Generally speaking, well-connected bike networks have smaller barriers to connectivity.

Most bicycle planners understand that a critical task in a network is to break the connectivity barriers. To help with this task, they need methods to identify and visualize barriers, both for their own analysis and design and for communicating with the public and other stakeholders. This study's objective was to develop a method for identifying and displaying barriers in low-stress bike networks, a method we hope will be a valuable tool in the qualitative assessment of a network's deficiencies.

Low-Stress Connectivity

Krizek and Roland analyzed the effect of discontinuities in on-street bicycle facilities on cyclist comfort and safety by surveying participants who bicycled through different kinds of breaks in the network (1). This work focused on a microscopic scale where discontinuities existed for a short section. It shows the effect of different types of

discontinuities in the on-street bike facility on a cyclist's perception of safety and comfort.

Birk and Geller found strong correlations between bicycle use and improvements made to the bicycle facilities at four key bridges that connect across the Willamette River in Portland, Oregon (2). Until those bridges were improved for cycling, the river was a major barrier between Portland's downtown and its largest residential areas. The large ridership gains that accompanied these improvements highlight the importance of breaching barriers as a main emphasis in bicycle network development.

Furth, Mekuria, and Nixon introduced the concept of a low-stress bike network, pointing out that when reasonable criteria are used to classify streets as high- or low-stress, and the high-stress segments that most people are unwilling to ride on are removed, the resulting network is often disconnected (3). They developed criteria for assigning four levels of traffic stress to street segments and crossings; however, the concept of low-stress connectivity can also be applied with other classification methods. Furth et al. defined a system-level measure of network connectivity: the number of origin–destination (O-D) pairs that are connected without undue detour (3). They also explored the concept of barriers within the

¹Department of Civil and Environmental Engineering, Northeastern University, Boston, MA

Corresponding Author:

Address correspondence to Theja Putta: pvvktheja@gmail.com

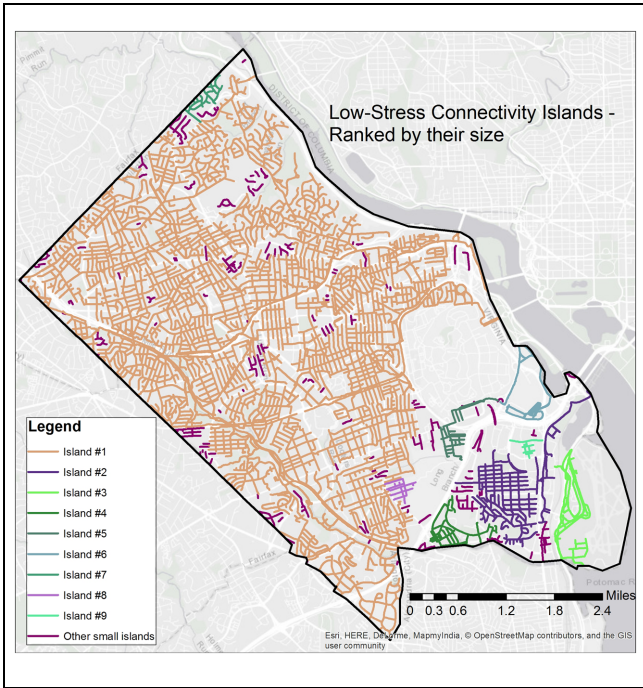


Figure 1. Low-stress connectivity islands for Arlington County, VA.

low-stress network. By using color to plot sets of connected segments, called “islands of connectivity,” they were able to identify barriers in a case study of San Jose. However, our experience with other cities has shown that visualizing gaps using connectivity islands works well only when the islands are neither too big nor too small. Large islands, in particular, can mask the long barriers within them. For example, Figure 1 shows the connectivity islands for Arlington County, VA. There is a large connectivity island covering much of the county, which might suggest excellent connectivity, however, there are significant barriers within that island (shown later in this paper).

Lowry and Hadden-Loh developed a method of measuring low-stress connectivity following the logic of geographic accessibility, measured as the number of desirable destinations that can be reached within a given distance of an origin (4). Because this measure is origin-based, it can be mapped to show regions of high and low accessibility. However, with such a measure it is not clear whether low accessibility is a result of network barriers or a lack of nearby destinations such as shops and restaurants.

Lowry, Furth, and Hadden-Loh developed the concept of centrality as a measure of a link’s importance: the number of O-D pairs whose shortest path includes that link (5). Comparing an ideal (future) bicycle network map with an existing map of low-stress bike routes, they used the before–after difference in a link’s centrality as a

means of prioritizing links. Links that breached an important barrier scored high by this metric.

The Dutch *Design Manual for Bicycle Traffic* (6) lists safety, comfort, attractiveness, cohesiveness, and directness as the key requirements for an effective bicycle network. The first three requirements can be seen as an elaboration of “low-stress,” and the last two as “connectivity.” With respect to cohesion, the key measure used in the Dutch guide is grid size or mesh size, which can be seen as the distance between parallel links in a network. They recommend a mesh size of 500 m for main bike routes in urban areas, and 1,000 to 1,500 m in rural areas. By these criteria, then, gaps in an urban bike network significantly wider than 500 m represent barriers on which network development should focus. Directness is measured as the ratio of actual trip length to the Euclidean distance for the same O-D pair.

If the bike network does not have a well-defined grid, mesh size is not a practical measure. Compared with an ideal density grid, a city’s low-stress network might have hundreds of gaps that exceed an ideal mesh size; which of the gaps is the most important? If the bike network is fragmented, directness loses its meaning, since the bike network might not even connect many trips. These issues point again to barriers, which directly affect a network’s cohesiveness and directness as a key concept for analyzing its deficiencies.

Barriers as the Negative of the Low-Stress Network

Although some barriers in a low-stress bicycling network are easy to identify, many are not obvious. Furth et al. highlight the variety of barrier types that can affect a low-stress bike network (3). These include natural barriers such as rivers and impassable hills; manmade linear barriers such as freeways, high-speed arterials, and railroads; large land parcels such as cemeteries, private developments, and even large parks that lack bike access; and discontinuities in the street network that may be artifacts of urban development.

The negative of the low-stress network is the “no-bicycling” space, which is a collection of polygons. A polygon that is part of a no-bicycling space can be considered a barrier if it spans a distance greater than a specified length: in our case studies we specified 600 m. A longer threshold is suitable for rural areas.

There will be several polygons in the no-bicycling space that do not meet the minimum span threshold, such as common city blocks; these smaller polygons are not significant barriers to bicycling. When they are deleted from the no-bicycling space, the remaining larger polygons form the barrier space. Figure 2 shows one such barrier polygon in Arlington, whose span, from its

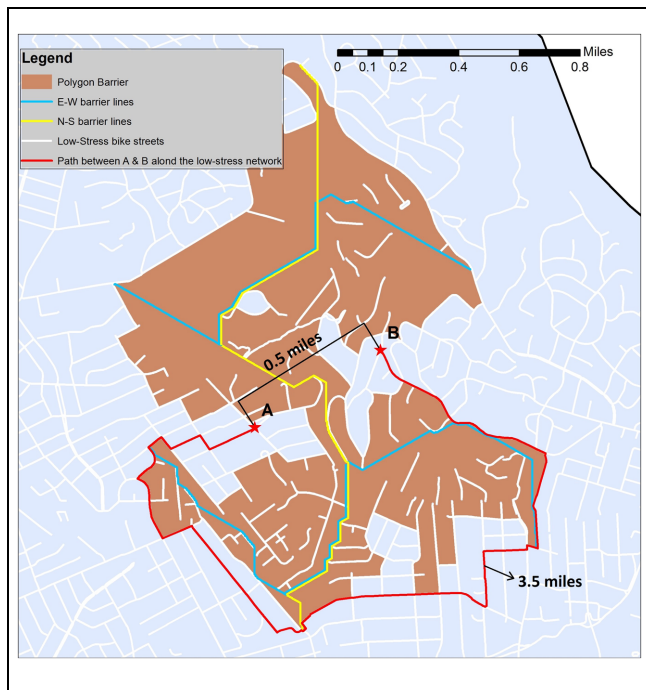


Figure 2. Polygon and polyline representation of a barrier in Arlington, VA.

extreme north point to its extreme south point, is 2 mi, which makes it a significant barrier to east–west travel. For example, the straight-line distance between points A and B is only 0.5 mi, but any low-stress route between these points must go around the barrier polygon. In this example, the shortest low-stress route from A to B is 3.5 mi, representing a level of detour that most cyclists will not accept.

Though a barrier polygon that is long, straight, and thin constitutes an obvious barrier to traveling along one axis, polygons with more complex shapes can represent multiple barriers, making it challenging to visualize effectively. For example, the barrier in Figure 2 has a shape that can be summarized roughly as an “I”: a central north–south barrier that inhibits east–west travel, and a pair of east–west barriers approximately a mile apart that inhibit north–south travel. The colored lines drawn in Figure 2 represent those barriers, and were generated using the methodology proposed in the next section.

The authors believe that for analysis and planning, barriers represented as lines are easier to understand than barrier polygons with complex shapes. Our objective, then, was to find a method to reduce barrier polygons to barrier lines, as shown in Figure 2. This task involved finding a balance between too many and too few lines. Having too many barrier lines will clutter the map with

near-duplicates, and insufficient barrier lines might result in some important barriers not being represented.

Methodology

This algorithm used the geographical boundary (polygon) and the low-stress bike network (lines) for the study area as inputs. A low-stress bike network is not limited to streets with separated bike infrastructure; it can also include mixed riding conditions that are low-stress resulting from low traffic volume and speed. In the case studies presented here, the stress classification was undertaken using a local adaptation of the criteria given in Furth et al. (3). The proposed algorithm generated a set of lines that represented the spatial barriers to the bike network.

The methodology can be divided into three main steps: 1) extract barrier polygons, 2) identify prominent points to serve as barrier line endpoints, and 3) draw barrier lines. Figure 3 gives an overview of the methodology. The methodology described in the following text is demonstrated using the low-stress bike networks in Boston, MA and Arlington, VA. The analysis and implementation of the algorithm was carried out using ArcGIS and python scripting.

Extract Barrier Polygons

In a network, streets are drawn as lines that typically represent their centerlines even though streets are actually polygons with a narrow width. Consequently, streets that end at the same intersection might not be represented as such. To avoid this potential misrepresentation, a small buffer was drawn around the low-stress bike network. Considering that local Boston streets tend to be 20 ft wide, we used a 20 ft buffer: large enough to bridge most inadvertent intersection gaps, but not so large as to obliterate real gaps.

The buffered bike network then becomes a set of polygons representing space that can be used for bicycling. Clipping or subtracting the buffered bike network from the boundary polygon results in the negative of the bicycling space or the “no-bicycling” zone, which is a collection of polygons, each of which is bounded by low-stress streets, the study area boundary, or both. Polygons that did not meet the minimum span threshold, discussed earlier, were discarded. The remaining polygons collectively form the barrier space, and represent true barriers to connectivity. Figure 4 shows the set of polygons that constitute the barrier space for the low-stress bike network of Arlington County. The low-stress streets are illustrated in white; the smaller polygons in the no-bicycling space that are not considered barriers are gray; and the barrier polygons are shown in a range of bold colors.

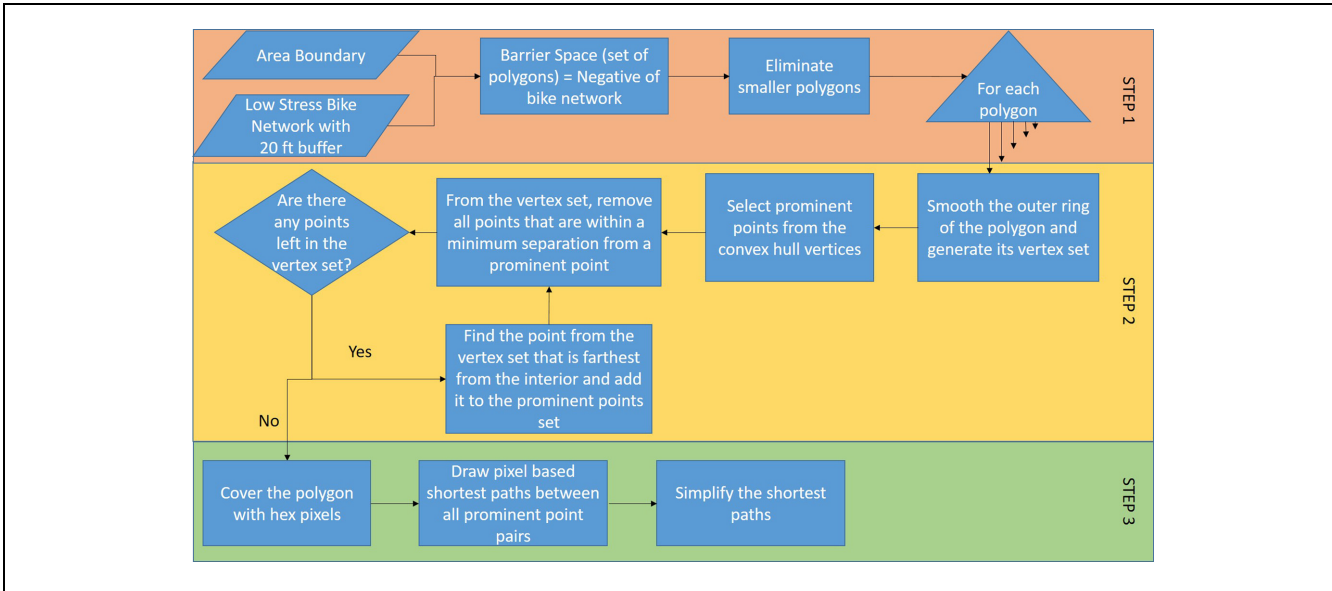


Figure 3. Proposed methodology for drawing barriers.

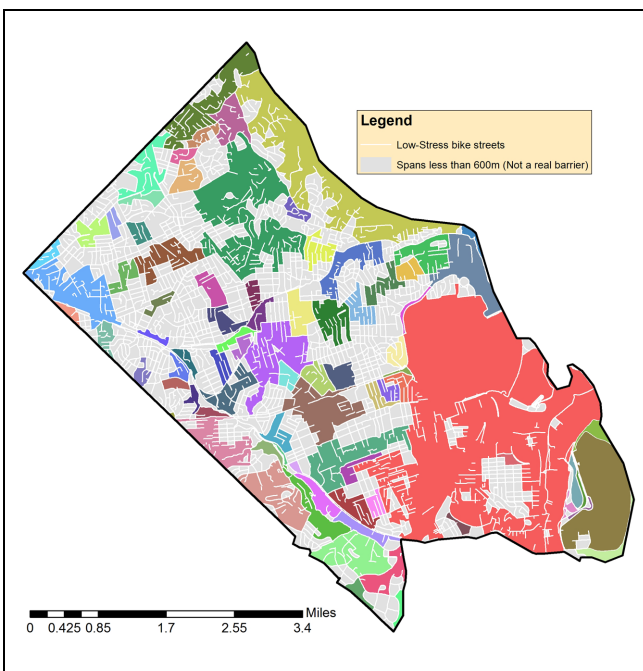


Figure 4. Barrier space in Arlington County, VA, consisting of multiple (colored) polygons.

Identify Prominent Points to Serve as Barrier Line Endpoints

The next step was to select a set of points (P) from each polygon's boundary that would form the ends of the barrier lines to be drawn. To get the longest possible barriers, the selected endpoints should be points that are "prominent" in the sense that they are far from the

interior of the polygon compared with other nearby points on the boundary. To avoid parallel duplicate barrier lines, prominent points should be separated by a distance greater than a minimum separation distance min_S chosen by the analyst. A longer min_S is desirable to avoid redundant barriers; however, with small polygons, a large value of min_S can result in missing meaningful barriers. To balance those concerns, in our case studies, we used a 1,600 m separation distance for large polygons, whereas for smaller polygons min_S was proportional to the polygon span, down to a minimum of 400 m (see Equation 1):

$$\text{min_S} = \min(1600, \max(0.4 * \text{span}, 400)) \quad (1)$$

where min_S = minimum separation distance (m) and span = polygon span.

Polygon Smoothing. Since prominent points must be on the polygon perimeter, they form a subset of the polygon's vertices. Owing to the complex shape of each polygon, the number of vertices on the perimeter can be large. This is especially true for polygons that have a lot of streets cutting into the perimeter, creating multiple "fingers" whose widths are twice the street buffer size (and thus 40 ft in our case studies). We reduced the number of vertices by filling in narrow fingers, thus smoothing the polygon boundary. This was accomplished by drawing a buffer around the perimeter that was slightly bigger than that of the streets (21 ft), and then removing the outermost 21 ft of the buffered polygon to conserve most of the original polygon boundary. The vertex set (V) from



Figure 5. Barrier polygon before and after smoothing.

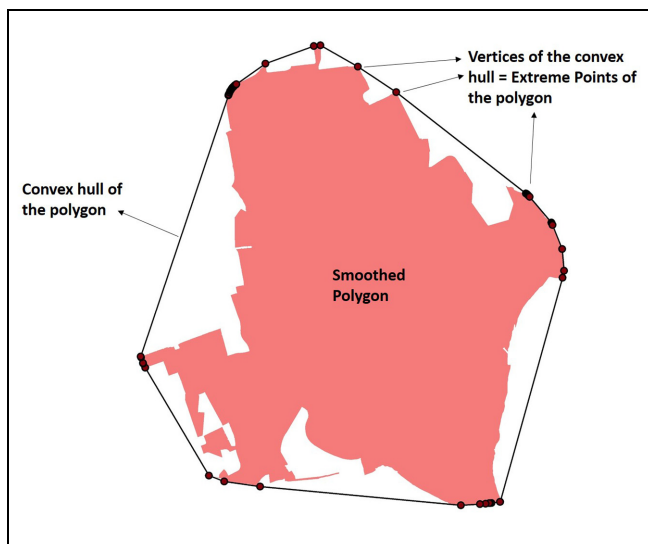


Figure 6. Smoothed polygon and its convex hull.

the perimeter of the smoothed polygon was smaller than that of the original polygon. Figure 5 shows the result of polygon smoothing compared with the original polygon for a barrier containing Arlington National Cemetery.

It is important to note that the smoothed polygon was only used to obtain the prominent points that serve as barrier endpoints. The original polygon was used as input for drawing the barrier lines.

Prominent Points and the Convex Hull. A starting point for selecting the set of prominent points is the set of extreme points of the polygon. For a two-dimensional polygon,

extreme points are points that cannot be expressed as a convex combination of any two other distinct points in the polygon, and thus tend to be farthest from the interior of the polygon. The extreme points of a polygon represent the V of its convex hull. If one were to stretch a large rubber band to surround all the points in the geometry and release it, the resulting shape when the rubber band becomes taut is the convex hull. Figure 6 shows the convex hull of the smoothed polygon.

If any side of the smoothed polygon was longer than $2 * \text{min_S}$, it was diced into segments of equal length and whose length was between min_S and $2 * \text{min_S}$. This dicing added vertices to the smoothed polygon boundary, and avoided the possibility of a gap greater than $2 * \text{min_S}$ between barrier endpoints.

To find a set of prominent points suitable for drawing boundaries, the set of extreme points had to be both reduced by eliminating points that lacked the minimum separation distance from a neighboring point and augmented by adding points where extreme points were too far apart.

If the shortest side of the convex hull was longer than the minimum separation, all vertices of the hull were chosen as prominent points. Otherwise, the following procedure was used to select the extreme points to be included in the set of prominent points. First, the span points (the two most distant extreme points) were selected. Extreme points within minimum separation distance from the span points were then eliminated and the convex hull redrawn.

Next, the shortest side of the convex hull was selected. If it was shorter than the minimum separation, at least

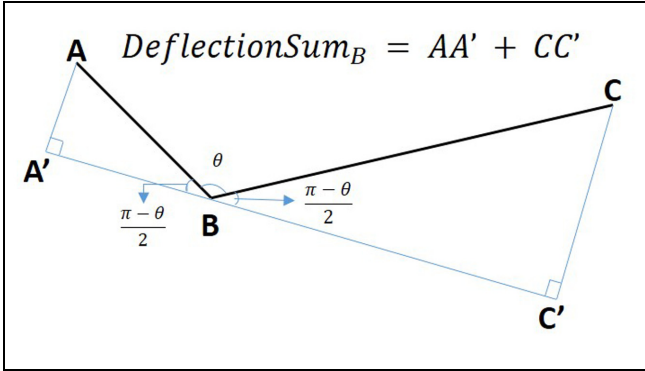


Figure 7. Illustration of deflection sum for a vertex.

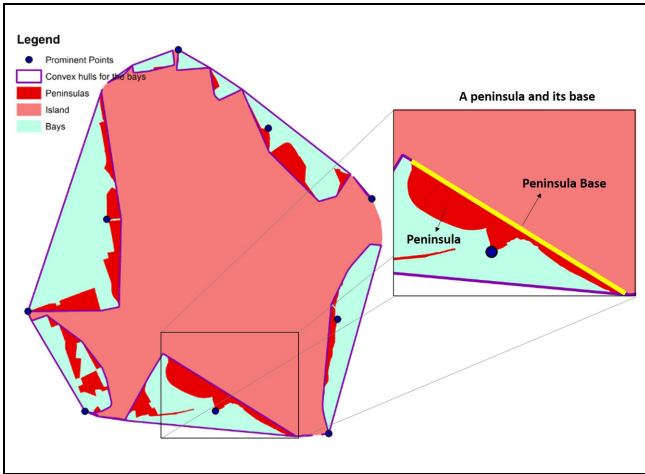


Figure 8. Bays, peninsulas, and peninsula bases of an island.

one of its vertices could not be selected. We eliminated the vertex with the smaller “deflection sum,” which was one-half the sum of deflections of the point’s incident edges, as shown in Figure 7. In that figure, consider point B, with incident edges AB and BC. Line A’C’ is drawn through point B bisecting the deflection angle between segments AB and BC. Segment CC’ is half the deflection involved in the turn from segment AB to BC, and segment AA’ is half the deflection involved in the turn from BC to AB. The deflection sum is the sum of the lengths of AA’, and CC’, and is given by

$$\text{DeflectionSum}_B = (\overline{AB} + \overline{BC}) * \sin\left(\frac{\pi - \theta_B}{2}\right) \quad (2)$$

where DeflectionSum_B is the deflection sum for point B, points A and C are its neighboring points, \overline{AB} and \overline{BC} are the lengths of segments AB and BC, and θ_B is the interior angle at B.

Once the vertex with the smaller deflection sum was eliminated, the hull polygon was redrawn with the

remaining vertices. The new shortest side was compared against the minimum separation and the process of eliminating vertices was repeated until the smallest side of the residual hull polygon was bigger than the minimum separation. The vertices left in the residual hull polygon were added to the prominent point set (P).

Next, if all the vertices of the smoothed polygon (V) were within a distance min_S of any prominent point, no more vertices were added to P. Otherwise, additional prominent points were chosen using of geoprocessing techniques explained in the following paragraphs.

Prominent Points from Peninsulas. If the smoothed perimeter of the polygon is thought of as the coastline of an island, the area between the perimeter and the convex hull can be viewed as bays. The convex hull of a given bay will overlap with part of the island; this overlap can be viewed as one or more peninsulas, which are essentially the parts of the islands that extend into the bays. Figure 8 shows the island, bays, and peninsulas for a polygon. Every vertex of the island belongs to the V of a peninsula or the convex hull of the island.

Each peninsula is connected to the rest of the island by a distinct line that can be called the peninsula base. For a vertex of a peninsula, the distance from the vertex to the peninsula base is a good measure of how far the point is from the interior of the island. For every point in V that was farther than min_S from all points in P, the distance to its corresponding peninsula base was calculated. The point that was farthest from its peninsula base was added to P. We then removed all points in V that were within a distance min_S of the newly added point. This process was repeated until there were no more points left in the set V.

The points in P formed the final set of prominent points and were used as the terminal points for drawing barrier lines. The prominent points selected for a polygon in Arlington using this method can be seen in Figure 8.

In the authors’ experience with applying this algorithm, the points generated adequately represented the vertices of the original polygon that were “prominent” in the general sense of being further from the interior of the polygon than any nearby point. However, if a large barrier polygon has a long “inlet” of bicycling space with a narrow mouth (e.g., a low-stress street penetrating deep into the polygon), exterior points on both sides of the inlet may be prominent in a general sense, but points on both sides may not be selected by the algorithm because of how the smoothing process closes narrow inlets. In such cases, which can happen only with a large polygon, an analyst could add a point manually.

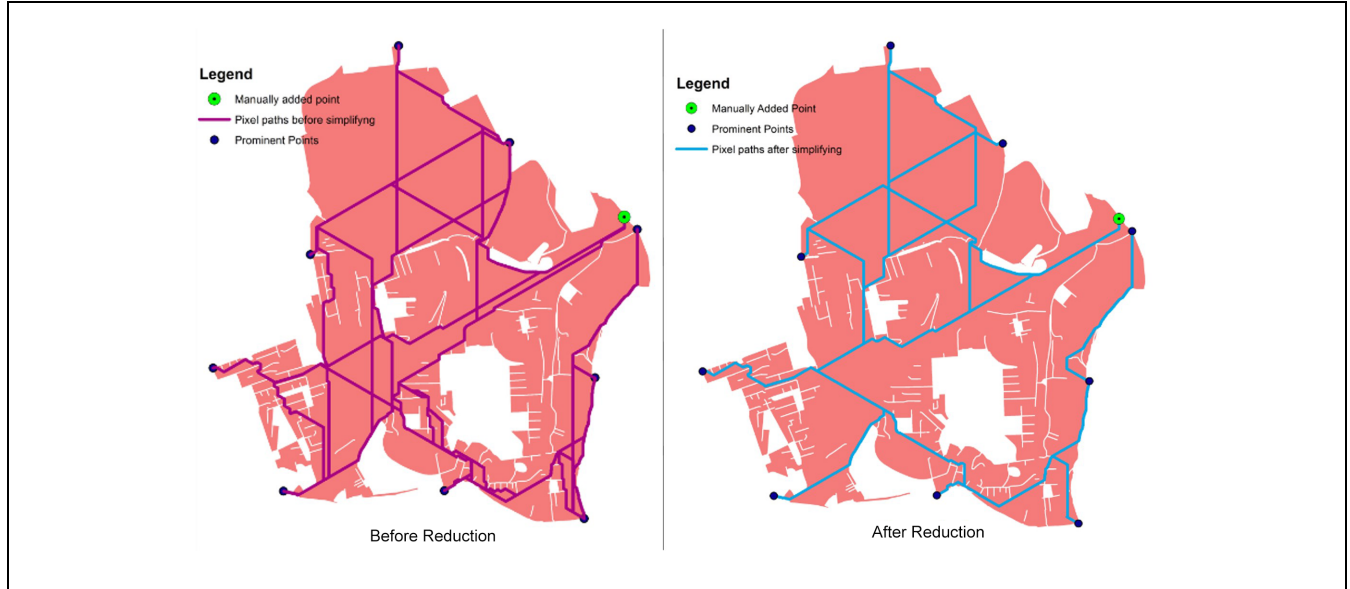


Figure 9. Pixel paths before and after reduction.

Draw Barrier Lines

The next step was to draw paths between all pairs of prominent points to represent barrier lines. A barrier line by definition should not intersect with any low-stress bike link, which means that it should remain within the barrier polygon, whose internal space is not solid but could contain many voids that represent bicycling space. Because of those voids, as well as a polygon's irregular edges, barrier lines often have to be curves or polylines, but for purposes of effective visualization should be as smooth as the geometry allows. Highly irregular voids and polygon edges can render a line-drawing heuristic that follows a direct line between endpoints until meeting a void or edge before seeking a path around the obstruction in a convoluted path that is not at all smooth to the eye.

Therefore, the approach we followed was to draw the shortest paths on a pixel grid. Hexagonal pixels were used for this as nearest-neighbor interaction is less ambiguous in a hex grid compared with a square grid. Birch, Oom, and Beecham suggest that hex grids are more suitable than square grids in connectivity and movement path applications (7). Although a square grid has the advantage of being described by two axes, a hex grid can also be described by two axes using axis transformation.

The barrier space was tessellated with equal-sized regular hexagon pixels such that none of the pixels were completely outside the barrier space and the entirety of the barrier space was covered by pixels. Pixel size should be small enough to ensure that no two adjacent pixels can bridge the buffer created by a low-stress street. Equation 3 shows the upper limit of pixel spacing p for a

given street buffer b , based on the geometry of similar hexagons that share an edge.

$$p < \sqrt{\frac{12}{13}} * b \quad (3)$$

For a 20 ft street buffer, p should not exceed 19.21 ft. Though a smaller pixel size could be used, this is computationally costly, so we used this upper limit as our pixel spacing.

Pixel Grid as a Graph. The hex pixel grid for a barrier polygon can be modeled as a graph with the pixel centroids as nodes and with each node having links to neighboring pixel centroids. For each prominent point in P , the pixel containing that point was the starting point. A breadth-first search of the graph generated the shortest paths on the pixel network to the all other points in P . This was repeated for all the points in P to get the pixel-based shortest paths between all pairs of prominent points.

Reducing the Pixel Paths. When overlaid on a map, the pixel-based shortest paths between prominent point pairs can be visually cluttered because of the irregular shape of the polygon's interior and exterior boundaries. Eliminating links from the shortest path network can reduce this clutter; however, it should be done in such a way that the resulting set of links still includes visually "reasonable" paths between prominent points.

The common cases that contribute to clutter are close parallel lines and dense lines that form small polygons.

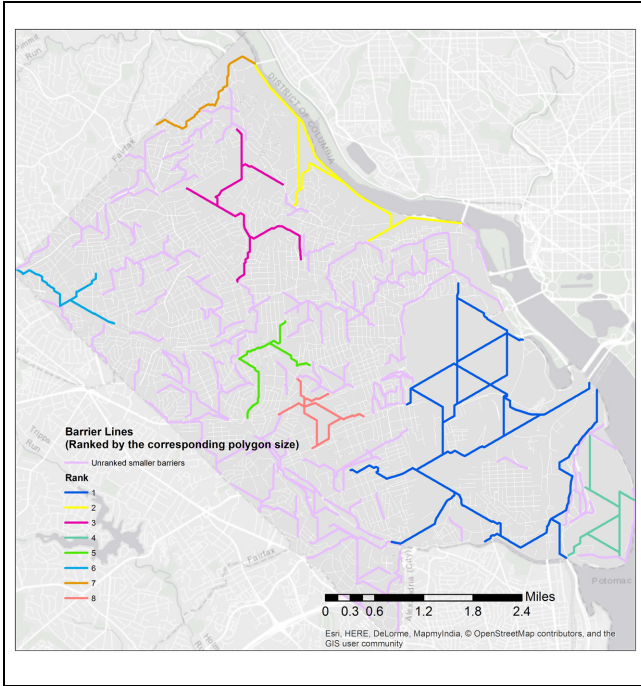


Figure 10. Barriers to low-stress bike network in Arlington, VA.

To reduce this clutter, we first modeled the shortest paths map as a planar graph, with nodes at the prominent points and wherever shortest paths intersected.

For an edge in the planar graph, if there was an alternative path between its endpoints, whose length was either less than 100 m longer than the edge or less than 1.5 times the edge length, then the edge was removed from the planar graph because its connecting function could be adequately replaced by the alternative path. If this elimination created any 2° node, it was eliminated by joining its incident edges. All the edges of the planar graph were treated in this manner, removing all the close parallels. Figure 9 shows both the original and reduced version of the pixel paths that represented the barrier lines.

Implementation on Real Networks

The algorithm was illustrated in two case study applications, Arlington County and Boston, whose low-stress bike networks were available to us from previous studies. The results may not reflect current conditions, because the network data do not include recent improvements.

Arlington County, Virginia

Figure 10 shows the barrier lines for Arlington ranked by size to highlight the larger barriers. The largest eight barriers are shown in distinct colors; smaller barriers are all shown in the same washed-out color. (Because small barriers can be located very close to one another, e.g.,

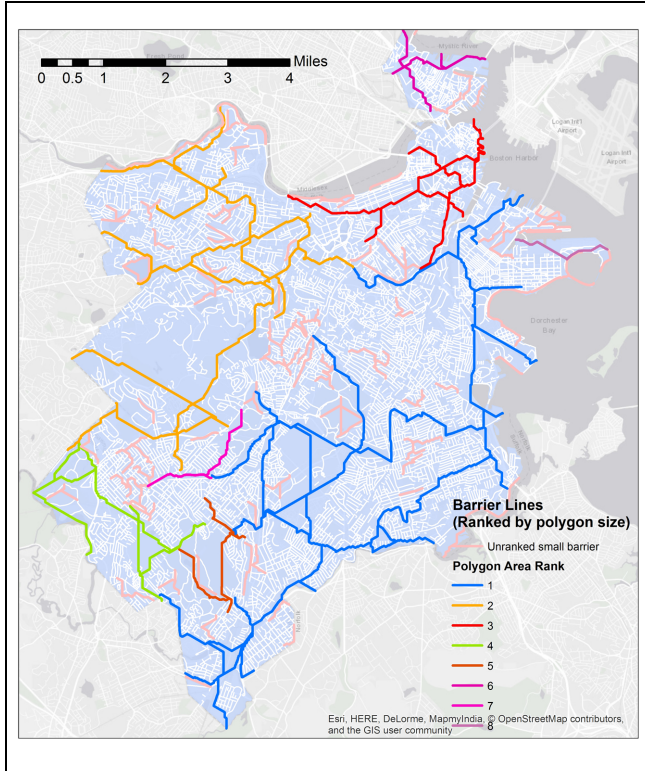


Figure 11. Barriers to low-stress bike network in Boston.

having endpoints on opposite sides of a low-stress street, they can appear to merge and thus be a long barrier; this is only an artifact of the figure's resolution.) The largest barrier includes Arlington National Cemetery, the Pentagon, Interstate 395, and U.S. Route 1, and spans 3.6 mi. The second biggest barrier is the Potomac River between Key Bridge and Chain Bridge, spanning 3.3 mi.

Recall the connectivity island shown in Figure 1; though it spans most of the county, it still contains many significant barriers that our method discovered, including a 1.9-mi barrier (from 17th Street N just west of Glebe Road to 35th Street N near Gulf Branch), a 1.3-mi barrier (from U.S. 50 N to 11th Street N), and 0.9 mi east-west barrier along Lee Highway (Edison Street to Nottingham Street). Though barriers that lie within a connectivity island do not disconnect a bike network completely, they can force long detours and thus break the network's functional connectivity.

Boston, Massachusetts

The study area for Boston also includes the town of Brookline, which is bordered by Boston on three out of four sides, and excludes East Boston, which is cut off from the rest of the city by Boston Harbor.

The eight biggest barriers for Boston are shown in Figure 11. Many of the barrier lines formed closed loops; surrounded areas like that are cut off from the rest of the

street network. These loops are connectivity islands, yet many have barriers within them, which our algorithm successfully mapped.

Wherever barriers come close to one another, it represents a “breach” in what would otherwise have been a far longer barrier. Such breaches can be very important links in a bike network. For example, the breaches between the biggest barrier (blue) and the second and third biggest barriers (orange and red) are the Southwest Corridor bike path and South Bay Harbor Trail. A breach can also be a quiet neighborhood street such as Sherrin Street and Bourneside Street, which might serve as a base for new local street bikeway.

Applicability and Limitations

The method presented here can be applied to rural, suburban, and urban bike networks. However, it is important that analysts select distance thresholds that are appropriate to the local density of the road network, so that detours that would be considered common or normal do not get classified as barriers.

For very sparse low-stress networks where nearly all space is a barrier, this method would be of little value. However, it could be of value even in places with a well-developed bike network, identifying barriers that may not be obvious.

Because the barrier lines drawn by our method follow a hex grid, they can create small, unnatural angles and irregularities. For public presentations, it may be worthwhile smoothing the lines further. Another weakness of the method is that the barriers it draws may not coincide exactly with features such as rivers, lakes, or freeways that are obvious barriers. The next generation model should incorporate a way to use known barrier lines or polygons supplied externally.

Conclusion

Being able to visualize barriers in a low-stress bicycling network is valuable for network planning. Although some barriers are obvious, others are not. Previous research identified the concept of connectivity islands; however, within the general area of a connectivity island, there can sometimes be long, significant barriers. We have developed a method that identifies and draws linear barriers in low-stress networks, dealing successfully with the complexities of street and low-stress network patterns. This method successfully found a balance between

drawing too many and too few barrier lines, yielding maps that were intuitive and that clearly showed gaps in the bicycling network that need to be addressed.

A visualization of the barriers in a low-stress network reveals the points where barriers come very close to one another; they represent breaches in what would otherwise be a much longer barrier, and as such could be valuable for bike network planning as the anchors of new routes to be developed.

Author Contributions

The authors confirm contribution to the paper as follows: study conception and design: PGF, TP; data collection: TP; algorithm development: PGF, TP; analysis and interpretation of results: TP, PGF; draft manuscript preparation: TP, PGF. Both authors reviewed the results and approved the final version of the manuscript.

References

1. Krizek, K. J., and R. W. Roland. What is at the End of the Road? Understanding Discontinuities of On-Street Bicycle Lanes in Urban Settings. *Transportation Research Part D: Transport and Environment*, Vol. 10, No. 1, 2005, pp. 55–68.
2. Birk, M., and R. Geller. Bridging the Gaps: How Quality and Quantity of a Connected Bikeway Network Correlates with Increasing Bicycle Use. Presented at 85th Annual Meeting of the Transportation Research Board, Washington, D.C., 2006.
3. Furth, P. G., M. C. Mekuria, and H. Nixon. Network Connectivity for Low-Stress Bicycling. *Transportation Research Record: Journal of the Transportation Research Board*, 2016. 2587: 41–49.
4. Lowry, M., and T. Hadden-Loh. Quantifying Bicycle Network Connectivity. *Preventive Medicine*, Vol. 95, 2017, pp. S134–S140.
5. Lowry, M., P. Furth, and T. Hadden-Loh. Prioritizing New Bicycle Facilities to Improve Low-Stress Network Connectivity. *Transportation Research Part A: Policy and Practice*, Vol. 86, 2016, pp. 124–140.
6. Rik de Groot, H. *Design Manual for Bicycle Traffic*. Crow, Ede, The Netherlands, 2016.
7. Birch, C. P. D., S. P. Oom, and J. A. Beecham. Rectangular and Hexagonal Grids Used for Observation, Experiment and Simulation in Ecology. *Ecological Modelling*, Vol. 206, No. 3–4, 2007, pp. 347–359.

The Standing Committee on Bicycle Transportation (ANF20) peer-reviewed this paper (19-01672).